

Estimation of FM Signal Parameters in Impulse Noise Environments

Igor Djurović, Ljubiša Stanković and Johann F. Böhme

Abstract— A simple algorithm based on discrete chirp Fourier transform (DCFT) is used for the chirp signal parameters estimation in impulse noise environments. A modification of the DCFT is introduced in order to produce accurate estimates in this case. This modification, called the robust DCFT, produces highly accurate results in impulse noise environments, while for the Gaussian noise it is only slightly worse than the standard one. Generalization to the parametric estimation of polynomial phase signals is given. It is based on the robust form of the integrated generalized ambiguity function (IGAF). We applied the IGAF-based procedure on the signal filtered by using the robust filter designed in the frequency domain.

I. INTRODUCTION

Numerous methods exist for frequency modulated (FM) signal parameters estimation in the Gaussian noise environment [1]-[4]. In particular, methods based on time-frequency (TF) analysis are proposed in [5]-[8] for linear FM (chirp) signal parameters estimation. Signal parameters are estimated by using projections of the TF representations along assumed instantaneous frequency lines. Other techniques are related to the fractional Fourier transform [9]-[11]. Third group of techniques is based on the signal auto-correlation function as a higher order ambiguity function [12]. In principle, most of the mentioned approaches can be reduced to the de-chirping and sinusoidal signal analysis. A simple de-chirping technique for discrete-time signals is proposed in [13]. It is based on the discrete chirp Fourier transform (DCFT). This technique can be understood as a discrete-time version of the maximum likelihood (ML) estimator for continuous-time signals from [4]. It has been shown in [13] that the maximum of side lobes, in the DCFT, is smallest for a prime number of considered samples. Therefore, the best

separation of close signal components in the parameter space, as well as high accuracy in the presence of significant amount of Gaussian noise, can be achieved for a sequence with prime lengths.

In numerous practical situations, noise environment cannot be modeled with the Gaussian probability density function (pdf). Namely, due to the natural disturbances (caused by atmospheric or underwater phenomena) or man-made disturbances (for example, effects in power lines), the resulting noise has very high values with a rare occurrence¹. These disturbances are usually modeled by long-tailed pdfs. Classical spectral estimators, like, for example, the Fourier transform (FT), or estimators of non-stationary signal spectra, such as the TF representations, are very sensitive to this kind of noise. Therefore, new approaches are required to handle parametric estimation of FM signal parameters in impulse noise environments. Fundamental approaches for handling data in impulse environments are proposed (or systematized) by Huber [14], [15]. Three basic groups of approaches for signal parametric estimation in impulse noise environments are proposed: M-, L- and R-estimates. In the case of M-estimates, a class of noises has been considered and the ML estimate for the noise from this class having the longest tail is used as the estimate for the entire class. This estimate is worse than any particular ML estimate for noises from the considered class, but it produces relatively accurate results for the entire class. For numerous classes considered in practice, the Laplacian noise is the worst one. Commonly, the M-estimate is designed as the ML estimate for the Laplacian noise environment. The L-estimates

¹Under high magnitude noise we assume disturbances several times larger than the signal amplitude.

are based on the order statistics. They are suitable for signal denoising and parametric estimation in mixed Gaussian and impulse noise environment. In the past 20 years these estimates have found numerous applications in signal processing. Important field for application of this concept is nonlinear filtering of digital images [16]. The R-estimates are based on the rank tests. Since this group of techniques is assumed to be computationally very demanding, with similar results as the L-estimate, it will remain outside the scope of this paper.

Based on the Huber's derivations, Katkovnik [17] developed the robust periodogram (i.e., the robust Fourier transform). Robust forms of the discrete unitary transforms and TF representations have been introduced recently [17]-[23]. These transforms are used for non-parametric spectral estimation.

Efficient methods for polynomial-phase FM signals parametric estimation are proposed for the Gaussian noise environment [1], [2], [13], [24], [25]. The goal of this paper is to develop techniques for parametric estimation of FM signals embedded in impulse noise environments. In the first step, an extension of the DCFT is proposed for parametric estimation of chirp signal parameters in impulse noise environments. In the next step, an approach based on the integrated generalized ambiguity function (IGAF) [24], has been modified for parametric estimation of higher order polynomial phase signals embedded in impulse noise environments. Note that the IGAF based approach is very efficient since two parameters are estimated in each algorithm stage, avoiding search over a large set of parameters. The L-filter form of DCFT and IGAF are used for estimation. Reasons for using L-estimates in this research are: (a) The resulting noise in the IGAF can be considered as a mixture of Gaussian and impulse noise, even for Gaussian input noise [20], [21]; (b) The M-estimates, that are robust to the impulse noise influence, can introduce spectral distortion, since they are commonly produced by a small number of signal samples. It is shown that the L-filter form produces accurate results for impulse noise environments, while its behavior

is similar to the standard one for the pure Gaussian noise [20], [21]. Analysis of multi-component signal estimation is performed, as well.

The paper is organized as follows. An overview of the robust FT forms is given in Section II. The DCFT and the proposed modification are considered in Section III. Generalization for the polynomial phase signals case is done in Section IV. Two forms of IGAF modification are proposed: one is based on the L-filter form of the kernel function, while in the other form impulse noise has been filtered in an initial stage by using the denoising technique from [26]. Numerical study covering different noise environments and multicomponent signals is presented in Section V. Concluding remarks are given in Section VI.

II. ROBUST FT

Consider a signal $x(n) = f(n) + \nu(n)$, where $f(n)$ is the useful signal component, while $\nu(n)$ is a white noise that can be of impulse nature, with statistically independent real and imaginary parts, $E\{\nu(n)\} = 0$, $E\{\text{Re}\{\nu(n)\}\text{Im}\{\nu(n)\}\} = 0$. Consider estimation of the useful signal's FT defined by:

$$\begin{aligned} F(k) &= \frac{1}{\sqrt{N}} \sum_{n=0}^{N-1} f(n)W_N^{nk} \\ &= \text{mean}\{\sqrt{N}f(n)W_N^{nk} | n \in [0, N)\}, \\ & \quad k \in [0, N), \end{aligned} \quad (1)$$

with $W_N = \exp(-j2\pi/N)$, based on noisy observations. The standard DFT of signal $x(n)$, $X(k) = \text{mean}\{\sqrt{N}x(n)W_N^{nk} | n \in [0, N)\}$, can be obtained as a solution of the following optimization problem:

$$\begin{aligned} X(k) &= \arg \min_m J(k; m), \\ J(k; m) &= \sum_{n=0}^{N-1} F(e(n, k; m)), \end{aligned} \quad (2)$$

where $F(e) = |e|^2$ is the loss function, while the error function is given by:

$$e(n, k; m) = \sqrt{N}x(n)W_N^{nk} - m. \quad (3)$$

Definition (2) is formally the same as the optimization problem employed for the moving average filter definition [16]. The standard DFT is the ML estimate of signal spectra for the Gaussian noise environment (in the same way as the output from the moving average filter is the ML estimate of the signal corrupted by the Gaussian noise).

However, both these linear solutions have poor accuracy for an impulse noise environment. This is the reason for introducing other loss function forms. Application of the loss function $F(e) = |e|$ results in the median filter [16]. The median filter output is the ML estimate of the signal corrupted by the Laplacian noise. In addition, this filter is a very accurate tool for almost all impulse noise environments. These facts have motivated application of the loss function $F(e) = |e|$ to the optimization problem defined by (2), (3). Due to the complex-valued nature of (2), (3), the robust M -DFT cannot be given in a closed form expression, but only in an implicit form [17], [18]:

$$X_R(k) = \frac{1}{\sum_{n=0}^{N-1} \frac{1}{|\sqrt{N}x(n)W_N^{nk} - X_R(k)|}} \times \sum_{n=0}^{N-1} \frac{x(n)W_N^{nk}}{|\sqrt{N}x(n)W_N^{nk} - X_R(k)|}. \quad (4)$$

For calculation of $X_R(k)$ it is necessary to use an appropriate iterative procedure.

In order to avoid handling the iterative procedures, a separable loss function

$$F(e) = |\operatorname{Re}(e)| + |\operatorname{Im}(e)| \quad (5)$$

is used in [19]. For minimization problem (2), and loss function (5) the marginal-median form of the DFT follows [19]:

$$\begin{aligned} & X_R(k) \\ &= \operatorname{median}\{\operatorname{Re}\{\sqrt{N}x(n)W_N^{nk}\} | k \in [0, N)\} \\ &+ j \operatorname{median}\{\operatorname{Im}\{\sqrt{N}x(n)W_N^{nk}\} | k \in [0, N)\}. \end{aligned} \quad (6)$$

Two reasons motivated introduction of the L-filter forms in the robust spectral analysis [26]:

- spectral distortion that can be introduced by the median-filter form (6). Reason for spectral

distortion is in the fact that in the robust FT realization the FT is replaced with one or two modulated signal samples;

- the L-filter can produce accurate spectra estimate for a mixture of the Gaussian and impulse noise environment.

The L-filter form of the DFT can be defined as [20], [21]:

$$X_L(k) = \sum_{n=0}^{N-1} a_n [\mathbf{r}_n(\mathbf{k}) + j\mathbf{i}_n(\mathbf{k})], \quad (7)$$

where $\sum_{n=0}^{N-1} a_n = 1$, $\mathbf{r}_n(\mathbf{k})$ and $\mathbf{i}_n(\mathbf{k})$ represent values from the sets $\mathbf{R}(\mathbf{k}) = \{\operatorname{Re}\{\sqrt{N}\mathbf{x}(\mathbf{n})\mathbf{W}_N^{n\mathbf{k}}\} | \mathbf{n} \in [0, \mathbf{N}]\}$ and $\mathbf{I}(\mathbf{k}) = \{\operatorname{Im}\{\sqrt{N}\mathbf{x}(\mathbf{n})\mathbf{W}_N^{n\mathbf{k}}\} | \mathbf{n} \in [0, \mathbf{N}]\}$, $\mathbf{r}_n(\mathbf{k}) \in \mathbf{R}(\mathbf{k})$, $\mathbf{i}_n(\mathbf{k}) \in \mathbf{I}(\mathbf{k})$, $n \in [0, N)$, sorted into nondecreasing order: $\mathbf{r}_i(\mathbf{k}) \leq \mathbf{r}_{i+1}(\mathbf{k})$, $\mathbf{i}_i(\mathbf{k}) \leq \mathbf{i}_{i+1}(\mathbf{k})$. For $a_n = 1/N$, for all $n = 0, 1, \dots, N-1$ this transform is reduced to the standard DFT, while for $a_{(N-1)/2} = 1$ and $a_k = 0$, for $k \neq (N-1)/2$ (odd N is assumed) it is reduced to the marginal-median form (6).

Here, we will use the α -trimmed form of the L-filter with coefficients a_n given by [20]:

$$a_n = \begin{cases} 1/[a(2-2N)+N], & n \in [(N-1)a, \\ & N-1-(N-1)a] \\ 0, & \text{elsewhere,} \end{cases} \quad (8)$$

where $a = 0$ produces the standard FT (1), while for $a = 0.5$ the median filter form (6) follows. Selected values of filter parameter a within the range $0 < a < 0.5$ can produce solution robust to both the Gaussian and impulse noise, avoiding spectral distortion effects.

III. ROBUST DISCRETE CHIRP-FT

A. Standard Discrete Chirp FT

Consider parameters estimation of a chirp signal,

$$f(n) = AW_N^{-nk_0 - n^2 l_0 - \varphi_0}, \quad n \in [0, N), \quad (9)$$

from noisy observations $x(n) = f(n) + \nu(n)$. We will assume that k_0 and l_0 are integers. Signal phase is denoted by φ_0 , $\varphi_0 \in [0, 2\pi)$.

The discrete chirp-FT defined in [13],

$$X_C(k, l) = \frac{1}{\sqrt{N}} \sum_{n=0}^{N-1} x(n) W_N^{n^2 l + nk},$$

$$(k, l) \in [0, N), \quad (10)$$

achieves maximum for the non-noisy signal (9) at the position corresponding to the signal parameters

$$(k_0, l_0) = \arg \max_{(k, l)} |X_C(k, l)|. \quad (11)$$

These parameters can be estimated for noisy signals by using the previous relation. A special case of the discrete chirp-FT is the discrete Fourier transform $X(k) = X_C(k, 0)$. Analysis of estimator (11) and its continuous time counterpart for Gaussian noise environment is given in [4], [6], [13], [27], [28]. This solution is not efficient in an impulse noise environment. In order to treat this kind of problems, here we propose the robust discrete chirp-FT.

B. Robust discrete chirp-FT

By analogy with the robust DFT, the robust L-filter form of the discrete chirp-FT can be defined as:

$$X_{LC}(k, l) = \sum_{n=0}^{N-1} a_n [\mathbf{r}_n(\mathbf{k}, \mathbf{l}) + \mathbf{j} \mathbf{i}_n(\mathbf{k}, \mathbf{l})], \quad (12)$$

where $\mathbf{r}_n(\mathbf{k}, \mathbf{l})$ and $\mathbf{i}_n(\mathbf{k}, \mathbf{l})$ represent values from the sets $\mathbf{R}(\mathbf{k}, \mathbf{l}) = \{\text{Re}\{\sqrt{N}x(n)W_N^{nk+n^2l}\} | n \in [0, N)\}$ and $\mathbf{I}(\mathbf{k}, \mathbf{l}) = \{\text{Im}\{\sqrt{N}x(n)W_N^{nk+n^2l}\} | n \in [0, N)\}$, $\mathbf{r}_n(\mathbf{k}, \mathbf{l}) \in \mathbf{R}(\mathbf{k}, \mathbf{l})$, $\mathbf{i}_n(\mathbf{k}, \mathbf{l}) \in \mathbf{I}(\mathbf{k}, \mathbf{l})$, $n \in [0, N)$, sorted into nondecreasing order: $\mathbf{r}_i(\mathbf{k}, \mathbf{l}) \leq \mathbf{r}_{i+1}(\mathbf{k}, \mathbf{l})$, $\mathbf{i}_i(\mathbf{k}, \mathbf{l}) \leq \mathbf{i}_{i+1}(\mathbf{k}, \mathbf{l})$. Here, we will use the weighting coefficients a_n given by (8), when $X_{LC}(k, l)$ is an α -trimmed mean.

The parameters estimate can be obtained from:

$$(\hat{k}_0, \hat{l}_0) = \arg \max_{(k, l)} |X_{LC}(k, l)|. \quad (13)$$

For $a_n = 1/N$, for all $n = 0, 1, \dots, N-1$, this transform is reduced to the standard DCFT (10).

C. Breakdown Point of the Algorithm

The breakdown concept is introduced in the robust estimation theory in [29]. For a finite number of samples it is the smallest percentage of observations that must be replaced by arbitrary values in order to force an estimator to produce values arbitrary far from the parameter values generated by non-noisy data. For standard transforms (DFT and DCFT) the breakdown point is $1/N$, since only one sample can make an arbitrary estimate. The breakdown point in the α -trimmed form is $\lceil (N-1)a + 1 \rceil / N$. Note that the breakdown point is the same for any L-filter form (with the same number of non-zero values of a_i) and the corresponding α -trimmed mean filter. Roughly speaking, it means that inaccurate results can be expected if probability of impulse appearance is higher than $\lceil (N-1)a + 1 \rceil / N$. In our application the real part of the resulting noise in (10) is given as:

$$\nu_{\text{Re}}(n; k, l) = \text{Re}\{\nu(n)\}$$

$$\times \cos(2\pi nk/N + 2\pi n^2 l/N) +$$

$$\text{Im}\{\nu(n)\} \sin(2\pi nk/N + 2\pi n^2 l/N). \quad (14)$$

A similar conclusion holds for the imaginary part. It can be seen that if the probability of impulses in both real and imaginary parts of the input noise is p , then the probability that impulses will affect resulting noise is $2p - p^2$. For example, it can be expected that a median form exhibits inaccurate behavior for $2p - p^2 \geq 0.5$, i.e., $p \geq 1 - \sqrt{2}/2$, while for $a = 1/4$ it is the case for $2p - p^2 \geq 0.25$, i.e., $p \geq 1 - \sqrt{3}/2$. These results are proven within the numerical study.

From this analysis it can be concluded that higher values of a produce representations more robust to the impulse noise influence. However, higher a means also that smaller number of signal samples is used to produce the estimate, and, therefore, it means higher spectra distortion. This effect is numerically analyzed in [26], where it is shown that for a very wide range of a , between two limit values $a = 0$ and $a = 0.5$, the results are satisfactory.

IV. POLYNOMIAL PHASE SIGNALS

A de-chirping procedure similar to that from Section III can be implemented for parametric estimation of general polynomial phase signals. Unfortunately, multidimensional search can be very demanding. This is the reason why numerous sub-optimal strategies are proposed in this area. Here, we will mention the method derived by Peleg, Porat and Friedlander [1], [30], [31], as well as the method presented in [2]. A modification of the integrated generalized ambiguity function (IGAF) [24] will be used in this paper for the parameter estimation of polynomial phase signals embedded in an impulse noise. Consider a polynomial phase signal:

$$f(n) = A \exp \left(j \sum_{m=0}^M a_m \frac{n^m}{m!} \right). \quad (15)$$

The signal is corrupted by a white noise $\nu(n)$ with independent real and imaginary parts, $x(n) = f(n) + \nu(n)$. Without loss of generality it will be assumed that the highest order of polynomial M is known in advance. In [24], the Gaussian noise environment is assumed, while we will here consider noise that can be of impulse nature². A generalized kernel function is defined recursively as:

$$\begin{aligned} K_x^M(n; \tau_1, \dots, \tau_{M-1}) \\ = K_x^{M-1}(n + \tau_{M-1}; \tau_1, \dots, \tau_{M-2}) \\ \times K_x^{(M-1)*}(n - \tau_{M-1}; \tau_1, \dots, \tau_{M-2}), \end{aligned} \quad (16)$$

and $K_x^1(n) = x(n)$ is the initial step. The IGAF is defined as:

$$\begin{aligned} P_x^M(g, h) \\ = \frac{1}{2} \sum_{\tau_1} \dots \sum_{\tau_{M-2}} |\mathcal{P}\{\cdot, \cdot; \tau_\infty, \dots, \tau_{M-\epsilon}\}|^2, \end{aligned} \quad (17)$$

²It has been shown in [20], [21] that resulting noise in the local auto-correlation function of signals corrupted by pure Gaussian noise can be considered as a mixture of the Gaussian and impulse noise. Then, the L-filter forms can produce more accurate spectra estimates than the standard forms. This effect is even more emphatic here, due to the higher order auto-correlations used for evaluation of the IGAF.

where:

$$\begin{aligned} \mathcal{P}\{\cdot, \cdot; \tau_\infty, \dots, \tau_{M-\epsilon}\} \\ = \sum_{\xi} K_x^{M-1}(\xi; \tau_1, \dots, \tau_{M-2}) \\ \times \exp(-j2^{M-2}(g\xi + h\xi^2/2)\Pi_{m=1}^{M-2}\tau_m). \end{aligned} \quad (18)$$

For non-noisy signal the IGAF $P_f^M(g, h)$ is maximized for $h = a_M$ and $g = a_{M-1}$. Therefore, the estimation of a_M and a_{M-1} can be performed as:

$$(\hat{a}_{M-1}, \hat{a}_M) = \arg \max_{(g, h)} P_x^M(g, h). \quad (19)$$

After de-chirping:

$$\begin{aligned} x^{(1)}(n) = x(n) \\ \times \exp \left(-j\hat{a}_M \frac{n^M}{M!} - j\hat{a}_{M-1} \frac{n^{M-1}}{(M-1)!} \right), \end{aligned} \quad (20)$$

the next two coefficients of the polynomial phase signal (a_{M-3}, a_{M-2}) can be estimated by using the IGAF $P_{x^{(1)}}^{M-2}(g, h)$. In this way, two coefficients of the polynomial phase signal are estimated in each algorithm stage. Unfortunately, error in estimation of the higher order coefficients propagates to the estimates of low order coefficients. For $M = 2$, the proposed approach can be reduced to the discrete chirp-FT. This method is very accurate. It approaches the Cramer-Rao lower bound derived in [32] for a relatively high amount of Gaussian noise [24], but it is sensitive to even small amount of impulse noise.

Two approaches for estimation of the polynomial phase signals parameters in the impulse noise can be employed. The first one is a straightforward extension of the robust DCFT approach, where, instead of $\mathcal{P}\{\cdot, \cdot; \tau_\infty, \dots, \tau_{M-\epsilon}\}$, we use:

$$\begin{aligned} \mathcal{P}_+(\cdot, \cdot; \tau_\infty, \dots, \tau_{M-\epsilon}) \\ = \sum_{n=0}^{N-1} a_n [\mathbf{r}_x(\mathbf{n}; \mathbf{g}, \mathbf{h}; \tau_1, \dots, \tau_{M-2}) \\ + j\mathbf{i}_x(\mathbf{n}; \mathbf{g}, \mathbf{h}; \tau_1, \dots, \tau_{M-2})], \end{aligned} \quad (21)$$

where $\mathbf{r}_x(\mathbf{n}; \mathbf{g}, \mathbf{h}; \tau_1, \dots, \tau_{M-2})$ and $\mathbf{i}_x(\mathbf{n}; \mathbf{g}, \mathbf{h}; \tau_1, \dots, \tau_{M-2})$ are elements from the sets

$$\{\text{Re}[K_x^{M-1}(\xi; \tau_1, \dots, \tau_{M-2})$$

$$\begin{aligned} & \times \exp(-j2^{M-2}(g\xi + h\xi^2/2)\Pi_{m=1}^{M-2}\tau_m), \\ & \xi \in [0, N] \end{aligned} \quad (22)$$

and

$$\begin{aligned} & \{\text{Im}[K_x^{M-1}(\xi; \tau_1, \dots, \tau_{M-2}) \\ & \times \exp(-j2^{M-2}(g\xi + h\xi^2/2)\Pi_{m=1}^{M-2}\tau_m)], \\ & \xi \in [0, N]\}, \end{aligned} \quad (23)$$

respectively, sorted in the nondecreasing order. Coefficients a_n given by (8) are used. The function $\mathcal{P}_{-1}(\cdot; \tau_\infty, \dots, \tau_{M-\epsilon})$ is applied in (17) instead of $\mathcal{P}(\cdot; \tau_\infty, \dots, \tau_{M-\epsilon})$. Then, the procedure can be conducted as in the previous cases. We will denote this form of the IGAF as $P_x^{M,a}(g, h)$. The main problem in this approach is in a low breakdown point of the algorithm. For example, consider $K_x^2(\xi; \tau_1) = x(\xi + \tau_1)x^*(\xi - \tau_1) = K_f^2(\xi; \tau_1) + r_{f\nu}(\xi; \tau_1)$, where $r_{f\nu}(\xi; \tau_1) = f(\xi + \tau_1)\nu^*(\xi - \tau_1) + \nu(\xi + \tau_1)f^*(\xi - \tau_1) + \nu(\xi + \tau_1)\nu^*(\xi - \tau_1)$. Let the impulse appearance probability in both real and imaginary part of noise $\nu(\tau)$ be p . Then, probability of impulse appearance in the resulting noise $r_{f\nu}(\xi; \tau_1)$ is $1 - (1-p)^4 = 4p - 6p^2 + 4p^3 - p^4$ for $\tau_1 \neq 0$. For example, if the input noise impulse probability is $p = 0.1$, the resulting noise will be influenced by impulse noise with probability of ≈ 0.34 . If the α -trimmed filter, with parameter a , is used to produce the robust estimate, then the breakdown point is the largest p that gives $4p - 6p^2 + 4p^3 - p^4 < a$. In the case of median-filter form of the IGAF, i.e., $a = 0.5$, the breakdown point is $p = 0.1591$, while for $a = 0.25$ it is only $p = 0.0694$. Note that the usage of higher order kernel functions causes decrease of the algorithm breakdown point. Namely, for $K_x^3(\xi; \tau_1, \tau_2)$ the breakdown point for $a = 0.5$ (median filter realization of the IGAF) is $p = 0.083$, while for $a = 0.25$ it is only $p = 0.0353$.

The second approach, that can be more accurate in this case, is based on the filtering (denoising) of FM signals in the first stage and on performing the standard IGAF based procedure for this signal. Three forms of the robust filters of signals with high frequency content are proposed so far:

- myriad and median filters admitting negative weights [33];

- robust filters designed in the frequency domain [26] and
- filters based on the minimax description length based thresholding in the wavelet domain [34].

Here, we will perform the robust filtering in the frequency domain based on the robust L-filter form of the DFT. The filtered signal can be calculated as:

$$\tilde{x}_L(n) = \frac{1}{\sqrt{N}} \sum_{k=0}^{N-1} X_L(k) W_N^{-nk}, n \in [0, N] \quad (24)$$

where $X_L(k)$ is the L-filter form of the DFT (7). In the next step, estimation of signal parameters is done, as in the case of the standard IGAF procedure. This IGAF form will be denoted by $\tilde{P}_x^{M,a}(g, h)$, where a is the corresponding parameter in the α -trimmed mean DFT form used in (24) for signal filtering. The main advantage of the proposed approach is in a higher breakdown point (the same as in the previously described robust DFT and robust DCFT based on the L-filter form) than in the case of the first approach.

V. NUMERICAL STUDY

A. Monocomponent Chirp Signal

Signal $f(n) = W_N^{-nk_0 - n^2 l_0}$, with $(k_0, l_0) = (12, 2)$, is assumed. Prime number $N = 67$ of samples is used. As the accuracy measure we have used the number of exact estimates of (k_0, l_0) parameters for various noises and various values of a in (8), in 100 trials. Numerical study of accuracy of the robust DCFT is performed for numerous noise environments, including the α -stable noise [35], mixed (contaminated) Gaussian noise [36], etc. For the sake of brevity, here we present results for the mixed Gaussian and Poisson noise environ-

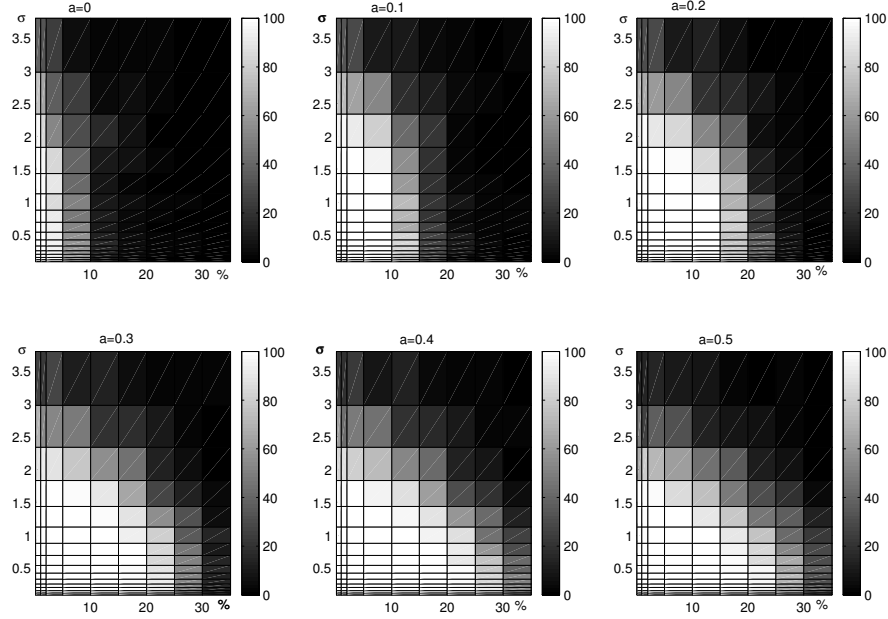


Fig. 1. Accuracy of the standard DCFT ($a = 0$) and robust DCFT forms for various $a = 0.1, 0.2, 0.3, 0.4, 0.5$. Accuracy measure is depicted in gray shades. Pure white represents accuracy in all 100 trials while pure black depicts no accurate trial.

ment³, when the resulting noise is given as:

$$\begin{aligned} \nu(n) = & \sigma[\nu_{G1}(n) + j\nu_{G2}(n)] \\ & + \nu_{P1}(n; p) + j\nu_{P2}(n; p), \end{aligned} \quad (25)$$

where $\nu_{G_i}(n)$, $i = 1, 2$ are mutually independent white Gaussian noises with unitary variance, $E\{\nu_{G_i}(n)\} = 0$, $i = 1, 2$ and $E\{\nu_{G_i}(n)\nu_{G_j}(n)\} = \delta(i - j)$, while $\nu_{P_i}(n; p)$, $i = 1, 2$ are mutually independent Poisson noises with probability of impulse appearance of p (probability of both positive and negative impulses is the same, $p/2$). In our numerical study we set impulses to be 5 times larger in magnitude than the useful signal amplitude.

Results obtained by using the standard DCFT ($a = 0$, the first column, the first row)

³This noise can be assumed as a special case from the Middleton class A of noises. Noises from the Middleton class A can be written as: $\nu_G(n) + \sum_{i=1}^Q u_i(n; \theta)$, where $u_i(n; \theta)$ is a waveform from interfering source and θ is a set of waveform parameters. It is commonly assumed that waveforms are emitted independently according to the Poisson pdf in time. Here we consider a single interfering waveform case $Q = 1$, distributed according to the Poisson pdf with amplitude significantly higher than the signal amplitude.

and the robust DCFT for $a = 0.1, 0.2, 0.3, 0.4$ and 0.5 are depicted in Fig.1. Pure white color means 100 accurate trials, while pure black color represents 0 accurate trials. It can be seen that the region of white color is the smallest for the standard DCFT. It is very narrow in the x -axis direction (axis of probability of impulse noise appearance), showing sensitivity of the standard approach to the impulse noise environment. Roughly speaking, white color region expands with the increase of a . Note that the results obtained with $a = 0.5$ are slightly worse than those obtained with $a = 0.4$, due to the spectra distortion effect. It can be seen that for a pure Gaussian noise (first column in the figures) results obtained by using the robust DCFT are only slightly worse (for high Gaussian environment) than those obtained by using the standard DCFT.

Realizations of the standard and the robust discrete chirp-FT form, in the case of Gaussian noise with $\sigma = 1$, and the Poisson noise for 15% of impulses, are shown in Fig.2. For the Gaussian noise, both the standard form for $a = 0$ and the robust form for $a = 0.4$, ex-

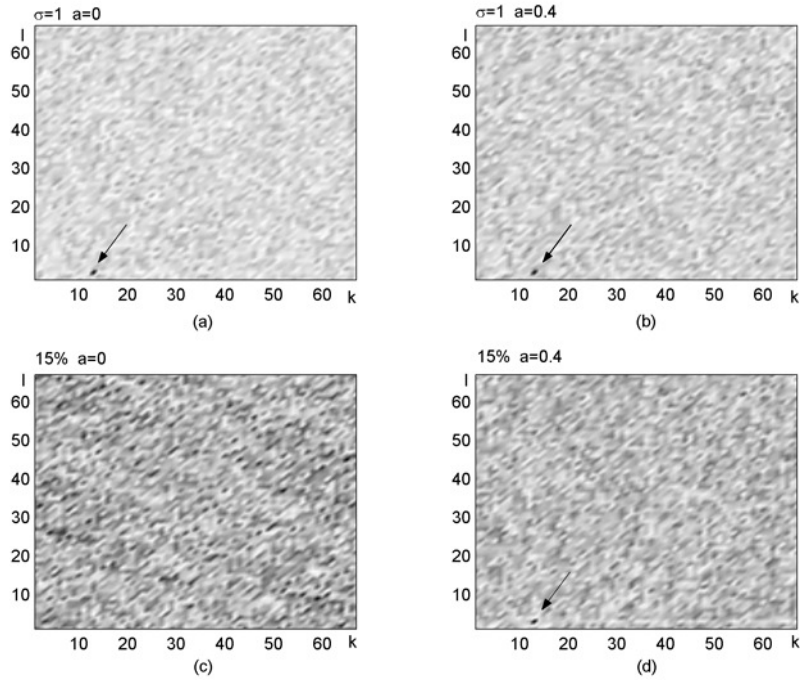


Fig. 2. Discrete chirp-FT $|X_L(k, l)|$ for monocomponent signal: (a) Gaussian noise $\sigma = 1$ and $a = 0$; (b) Gaussian noise $\sigma = 1$ and $a = 0.4$; (c) Poisson noise 15% and $a = 0$; (d) Poisson noise 15% and $a = 0.4$.

hibit clear maxima of $|X_L(k, l)|$ at the correct position (k_0, l_0) . However, it can be observed that the standard transform behaves slightly better, i.e., values of $|X_L(k, l)|$ outside (k_0, l_0) are higher in the case of the robust form than in the case of the standard one. In the second example for the Poisson noise, the standard discrete chirp-FT is useless, Fig.2c. In this case the robust form is still accurate, with position of the true maximum being clearly emphasized, Fig.2d.

B. Multicomponent Chirp Signals

In this group of experiments we considered three- and four-component signal cases:

$$x(n) = \sum_{i=0}^{m-1} W_N^{-nk_{im} - n^2 l_{im}}. \quad (26)$$

For three-component signal, $m = 3$, parameters are $(k_{i3}, l_{i3}) = (12, 2), (49, 35), (18, 24)$. In the case of a four-component signal, $m = 4$, we assumed $(k_{i4}, l_{i4}) =$

$(44, 57), (36, 65), (53, 10), (55, 12)$. A four-component signal case is shown in Fig.3. Similar conclusions as in the case of monocomponent signals can be drawn from these figures. Namely, in the case of a pure Gaussian noise (see Fig.3a), the standard DCFT produces clear peaks corresponding to parameters of the signal components. These peaks can also be recognized in the case of the robust DCFT form (dark spots marked with arrows) Fig.3b. In the case of impulse noise, the standard DCFT produces poor results (Fig.3c) since we cannot recognize peaks that correspond to the signal components. In the case of robust counterpart of this transform, the signal components can be easily seen. These facts confirm our previous considerations. The robust forms are slightly worse than the standard form in the case of a pure Gaussian noise. In impulse noise the standard DCFT is useless, while the robust forms behave accurately.

In order to reaffirm these conclusions we present numerical analysis of the DCFT forms

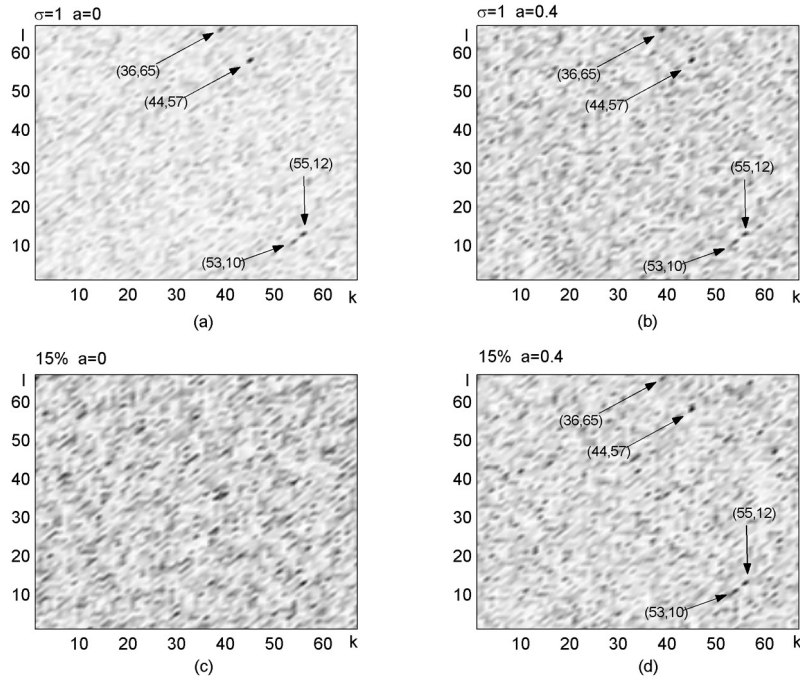


Fig. 3. Discrete chirp-FT $|X_L(k, l)|$ for multicomponent signal: (a) Gaussian noise $\sigma = 1$ and $a = 0$; (b) Gaussian noise $\sigma = 1$ and $a = 0.4$; (c) Poisson noise 15% and $a = 0$; (d) Poisson noise 15% and $a = 0.4$.

for noise environments. Ratio between its mean value at the true signal positions, in parameter space (k_{im}, l_{im}) , and the mean value in the entire (k, l) plane:

$$B = \frac{\frac{1}{m} \sum_{i=0}^{m-1} |X_{LC}(k_{im}, l_{im})|}{\frac{1}{N^2} \sum_{k,l} |X_{LC}(k, l)|}, \quad (27)$$

is used as a quality measure of the DCFT forms. This ratio is evaluated for the Gaussian and Poisson noise in Monte-Carlo simulation with 100 trials. The left column of Fig.4 depicts results obtained for three-component signal, while corresponding results for the four-component signal are given in the right column. The first row (Figs.4a,b) presents results for pure Gaussian noise. It can be seen that the best results are produced for the standard form. Also, it can be noted that the ratio B decreases as a increases, i.e., worse results are achieved for the α -trimmed forms with higher a . In the case of Poisson noise (Figs.4c,d) the standard discrete chirp-FT pro-

duces the worst ratio B . Only in the range of a small impulse noise probability (less than 1%) it is better than the robust forms. Note that in this case 1% of impulses is smaller than the breakdown point of the standard transform, that exhibits $1/N = 1/67$. For higher p it behaves poorly. Reason why the standard form could produce better results for very small percentage of impulse noise appearance is in nonlinearity introduced by the robust methods. Ratio B , as a function of a , is depicted in Fig.4e-h. Three and four component signal cases, for pure Gaussian noise environment and a fixed signal to noise ratio, are given in Figs.4e and 4f, respectively. It can be seen that B decreases almost linearly for $SNR = 20\text{dB}$ and $SNR = 0\text{dB}$, while for very high noise, $SNR = -20\text{dB}$, the obtained ratio is almost constant. In the case of a pure Poisson noise (depicted results are obtained for $p = 1\%$, $p = 10\%$, $p = 25\%$ and $p = 35\%$) ratio B increases to the breakdown point, corresponding to the considered noise case, and

after that it slightly decreases, Figs.4g and 4h. However, for a wide range between the breakdown point and $a = 0.5$, results are almost the same. From Figs.4g and 4h can be noticed that the standard DCFT produces better results for $p = 1\%$ of impulses than robust counterparts with $a > 0.25$. It can be concluded from Figs.4g and 4h that in impulse noise environments, with at least several percents of impulses, good empirical value of parameter a could be anywhere within $a \in [0.25, 0.45]$. However, a question how precisely to select parameter a in the α -trimmed mean form of the robust DCFT in order to obtain the best results, remains to be addressed. It is an important issue in all techniques based on the robust statistics methods. An approach proposed by [37] has been recently applied in [38] for selection of the parameter a in signal denoising based on the robust FT. Obtained results are encouraging. Our plan is to apply them in the case of robust DCFT.

C. IGAF - Monocomponent signal

Consider a signal with cubic phase:

$$f(n) = \exp(ja_3n^3/6 + ja_2n^2/2 + ja_1n + ja_0), \quad (28)$$

with $N = 128$ samples and coefficients $a_3 = 48/N^3$, $a_2 = 48/N^2$, $a_1 = 12/N$, and $a_0 = 0$. The signal is corrupted by Gaussian noise with variance $\sigma^2 = 1$. The standard IGAF, $P_x^{3,0}(g, h)$, the median-based form $P_x^{3,1/2}(g, h)$, and the α -trimmed form for $a = 3/8$, $P_x^{3,3/8}(g, h)$ are depicted in Figs.5a-c. Functions are evaluated over a grid $g = i/N^2$ and $h = j/N^3$, where $i, j \in [0, N]$. It can be easily concluded that these three forms produce results of the same accuracy. Namely, peak depicted in dark shades, representing the true signal parameters in the parameter space, can be easily seen in all three cases. The second considered case was signal embedded in the Poisson noise with 10% impulses in both real and imaginary part. The IGAF forms for this noise are shown in Figs.5d-f. The standard IGAF is useless in this case, while two other forms produce quite accurate results. Note that in this case similar results can be obtained by using the IGAF form with application of

the robust pre-filter.

We checked the performance of the IGAF forms for a mixture of Gaussian and impulse noise. The amount of Gaussian noise is fixed to $\sigma^2 = 0.25$, while the impulse noise is varied within the range [0%, 25%]. Results are depicted with black lines in Fig.6 for 25 independent trials. Results obtained with these forms of the robust IGAF are denoted with v_1 . Note that, due to the used calculation method (g and h are calculated over a grid where the exact values are located), these results are only description of the general algorithm behavior, but not a detailed statistical analysis. From the figure it can be seen that even for a small amount of impulse noise the new IGAF performs better than the standard one. Note that estimation of the parameter a_3 is more accurate than the estimation of a_2 . This fact is analyzed in [24]. In the impulse noise case we could not get so high robustness to the impulse noise as in the case of discrete robust DCFT. Namely, the kernel used in this example, $K_x^2(\xi; \tau_1) = x(\xi + \tau_1)x^*(\xi - \tau_1)$ in (21), has twice more impulses than the signal $x(\xi)$. Thus, situation is worse in the case of higher order kernels. In order to improve results we applied signal pre-filtering with a robust filter in the frequency domain. These results are denoted as v_2 , i.e., with gray lines in Fig.6. Comparing results with the first form of the robust IGAF, a significant improvement in accuracy (lower MSE) may be observed.

D. IGAF - Multicomponent signal

Consider a two-component signal:

$$\begin{aligned} f(n) &= \exp(ja_{31}n^3/6 + ja_{21}n^2/2 + ja_{11}n + ja_{01}) \\ &+ \exp(ja_{32}n^3/6 + ja_{22}n^2/2 + ja_{12}n + ja_{02}) \end{aligned} \quad (29)$$

corrupted with the same noises as in the case from Fig.5. Signal parameters are $a_{31} = 48/N^3$, $a_{21} = 48/N^2$, $a_{11} = 12/N$, $a_{01} = 0$, $a_{32} = 24/N^3$, $a_{22} = 24/N^2$, $a_{12} = 12/N$, and $a_{02} = 0$. Results are depicted in Fig.7. It can be seen that in the Gaussian noise environment all IGAF forms perform with similar accuracy, while in the impulse noise only the

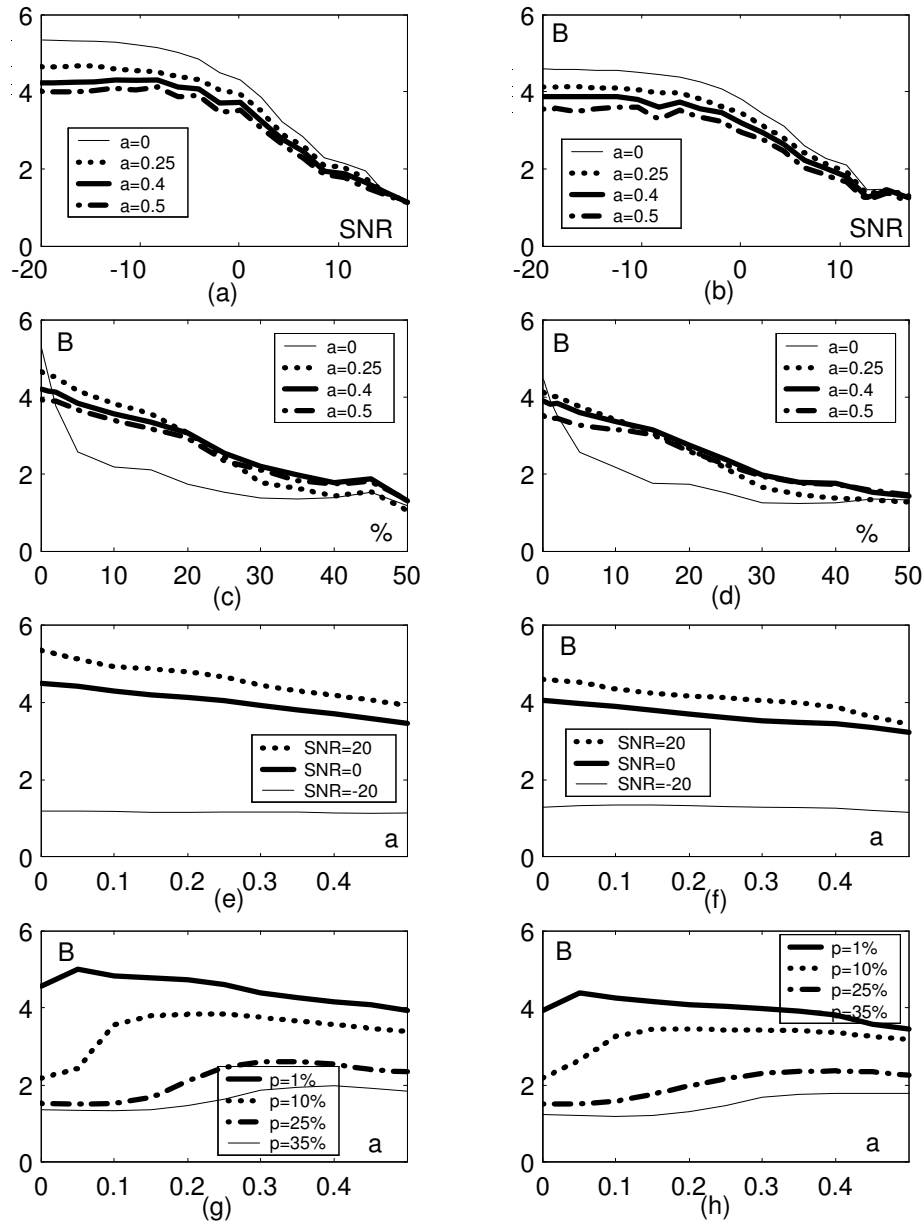


Fig. 4. Ratio B for: (a) Three-component signal and Gaussian noise as a function of SNR; (b) Four-component signal and Gaussian noise as a function of SNR; (c) Three-component signal and Poisson noise as a function of impulse probability p ; (d) Four-component signal and Poisson noise as a function of impulse probability p ; (e) Three-component signal and Gaussian noise as a function of a ; (f) Four-component signal and Gaussian noise as a function of a ; (g) Three-component signal and Poisson noise as a function of a ; (h) Four-component signal and Poisson noise as a function of a .

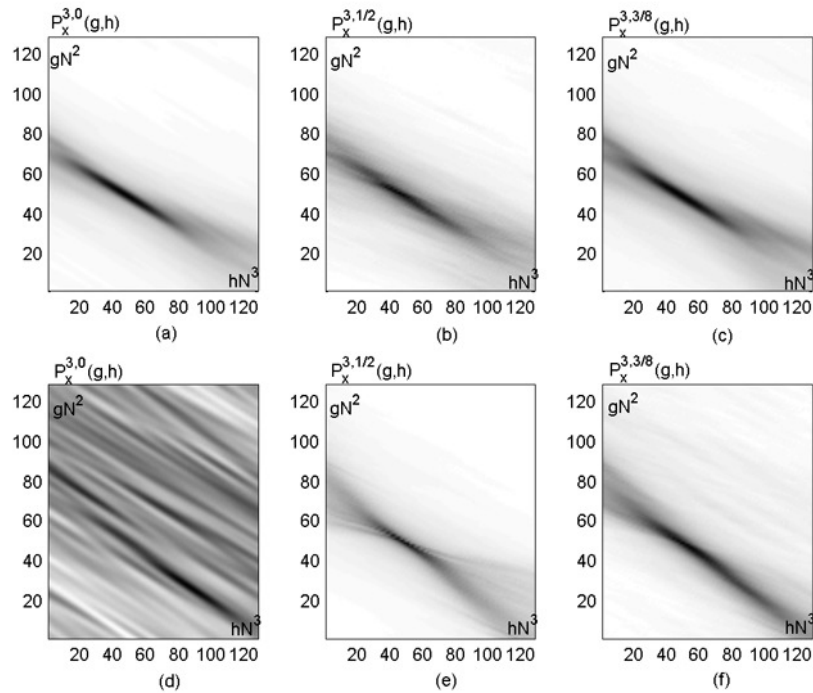


Fig. 5. IGAF function for monocomponent signal: First row - Gaussian noise environment; Second row - Impulse noise environment; First column - standard IGAF $P_x^{3,0}(g, h)$; Second column - median based $P_x^{3,1/2}(g, h)$; Third column - α -trimmed form $P_x^{3,3/8}(g, h)$.

IGAF form $P_x^{3,3/8}(g, h)$ performs in a satisfactory manner. Namely, the marginal-median form, due to the nonlinearity, doesn't produce so good resolution to separate signal components in the parameter space.

VI. CONCLUSION

Robust discrete chirp-FT is proposed in this paper. It is a very accurate tool for the chirp signal parameters estimation in impulse noise environments. Performance of this transform is evaluated for various noise environments. It is shown that the transform with parameter a , corresponding to higher robustness, performs better in heavier impulse noise environments. However, the largest values of a , close to $a = 0.5$, introduce spectra distortion, causing slightly less accurate results comparing to those obtained with $a < 0.5$. We have generalized this approach to the higher-order polynomial phase signals. Since de-chirping proce-

dures can be very demanding, we have used approach based on the robust form of the IGAF. Again, the α -trimmed forms behave better than the standard one in impulse noise environments. At the same time, they are better than the marginal-median form in the case of multicomponent signals. In order to decrease breakdown point in the IGAF based estimator, the robust pre-filtering is performed in the first algorithm stage. Adaptive techniques for selecting parameter a in the α -trimmed mean based estimators will be the topic of our further research.

REFERENCES

- [1] S. Peleg and B. Porat, "Estimation and classification of signals with polynomial phase," *IEEE Trans. Inf. Th.*, Vol. 37, 1991, pp. 422-430.
- [2] P. M. Djurić and S. M. Kay, "Parameter estimation of chirp signals," *IEEE Trans. ASSP*, Vol. 38, No.12, Dec. 1990, pp. 2118-2126.
- [3] E. J. Kelly, I. S. Reed and W. L. Root, "The detection of radar echoes in noise Part I," *Jour.*

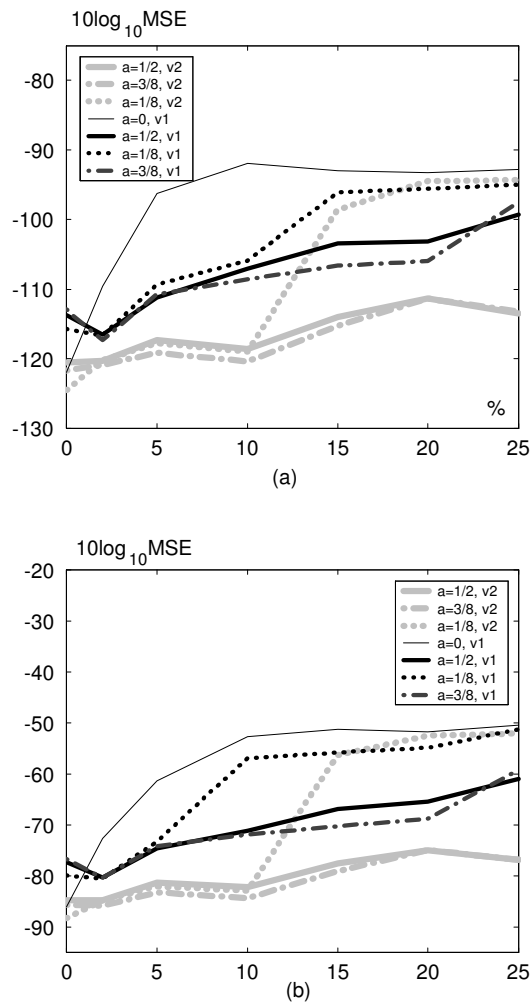


Fig. 6. MSE of parametric estimation for two highest coefficients: (a) a_3 estimation; (b) a_2 estimation. Black lines - estimation accuracy for IGAF function filtered with L-filter forms; Gray lines - estimation accuracy for IGAF procedure applied to signal filtered with L-filter based robust filter. Thin line - Standard approach; Thick solid line - Marginal-median IGAF; Dotted line - $a = 1/8$; Dash-dot line - $a = 3/8$.

- Soc. Ind. Appl. Math.*, Vol. 8, June 1960, pp. 309-341.
- [4] E. J. Kelly, I. S. Reed and W. L. Root, "The detection of radar echoes in noise Part II," *Jour. Soc. Ind. Appl. Math.*, Vol. 8, Sep. 1960, pp. 481-507.
- [5] S. Barbarossa and O. Lemoine, "Analysis of non-linear FM signals by patterns recognition of their time-frequency representation," *IEEE Sig. Proc. Let.*, Vol. 3, No.4, Apr. 1996, pp. 112-115.
- [6] J. C. Wood and D. T. Barry, "Radon transformation of time-frequency distributions for analysis of multicomponent signals," *IEEE Trans. Sig. Proc.*, Vol. 42, No.11, Nov. 1994, pp. 3166-3177.
- [7] S. Barbarossa, "Analysis of multicomponent LFM signals by a combined Wigner-Hough transform," *IEEE Trans. Sig. Proc.*, Vol. 43, No.6, June 1995, pp. 1511-1515.
- [8] B. Ristić and B. Boashash, "Kernel design for the time-frequency signal analysis using the Radon transform," *IEEE Trans. Sig. Proc.*, Vol. 41, No.5, May 1993, pp. 1996-2008.
- [9] S.-C. Pei and J.-J. Ding, "Relations between fractional operations and time-frequency distributions, and their applications," *IEEE Trans. Sig. Proc.*, Vol. 49, No.9, Aug. 2001, pp. 1638-1655.
- [10] L. B. Almeida, "The fractional Fourier transform and time-frequency representations," *IEEE Trans. Sig. Proc.*, Vol. 42, No.11, Nov. 1994, pp. 3084-3091.
- [11] T. Alieva and M. J. Baastians, "Wigner distribution and fractional Fourier transform," in *Proc. Sig. Proc. Appl.*, Vol. 1, 2001, pp. 168-169.
- [12] S. Barbarossa, A. Scaglione and G. B. Giannakis,

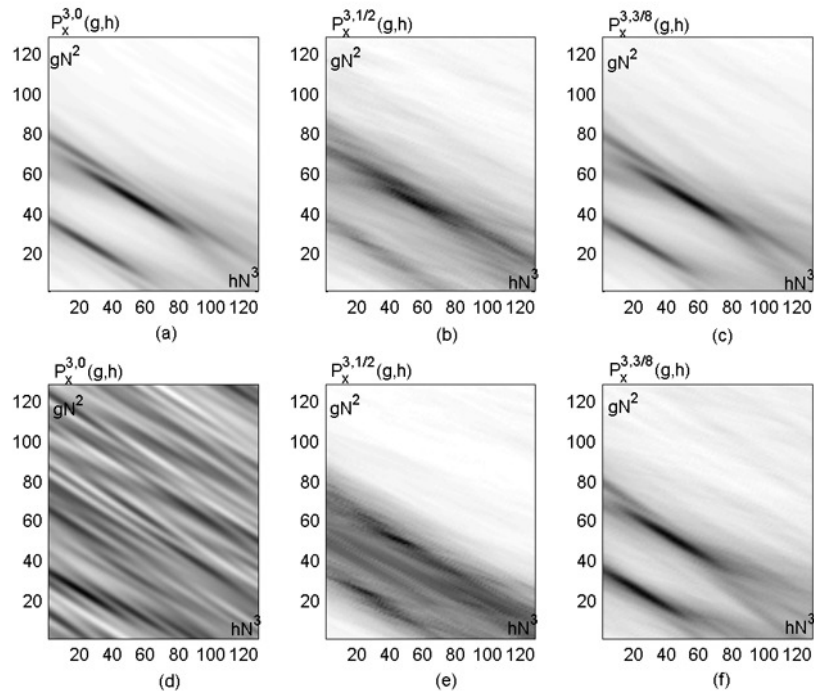


Fig. 7. IGAF function for monocomponent signal: First row - Gaussian noise environment; Second row - Impulse noise environment; First column - standard IGAF $P_x^{3,0}(g, h)$; Second column - median based $P_x^{3,1/2}(g, h)$; Third column - α -trimmed form $P_x^{3,3/8}(g, h)$.

- “Product high-order ambiguity function for multicomponent polynomial-phase signal modeling,” *IEEE Trans. Sig. Proc.*, Vol. 46, No.3, Mar. 1998, pp. 691-708.
- [13] X.-G. Xia, “Discrete chirp-Fourier transform and its application to chirp rate estimation,” *IEEE Trans. Sig. Proc.*, Vol. 48, No.11, Nov. 2000, pp. 3122-3133.
- [14] P. J. Huber, *Robust statistics*, John Wiley&Sons, 1981.
- [15] P. J. Huber, “Robust regression: Asymptotics, conjectures and Monte Carlo,” *Ann. Math. Statist.*, Vol. 1, No.5, 1973, pp. 799-821.
- [16] I. Pitas and A. N. Venetsanopoulos, “Order statistics in digital image processing,” *Proc. IEEE*, Vol. 80, No.12, Dec. 1992, pp. 1893-1992.
- [17] V. Katkovnik, “Robust M-periodogram,” *IEEE Trans. Sig. Proc.*, Vol. 46, No.11, Nov. 1998, pp. 3104-3109.
- [18] V. Katkovnik, “Robust M-estimates of the frequency and amplitude of a complex-valued harmonic,” *Sig. Proc.*, Vol. 77, No.1, Aug. 1999, pp. 71-84.
- [19] I. Djurović, V. Katkovnik and LJ. Stanković, “Median filter based realizations of the robust time-frequency distributions,” *Sig. Proc.*, Vol. 81, No.7, July 2001, pp. 1771-1776.
- [20] I. Djurović, LJ. Stanković and J. F. Böhme, “Estimates of the Wigner distribution in Gaussian noise environment,” *AEU International Journal of Electronic Communications*, Vol. 56, No.5, 2002, pp. 337-340.
- [21] I. Djurović, LJ. Stanković and J. F. Böhme, “Robust L -estimate based forms of the signal transforms and TF representations,” *IEEE Trans. Sig. Proc.*, Vol.51, No.7, July 2003, pp. 1753-1761.
- [22] V. Katkovnik, I. Djurović and LJ. Stanković, “Instantaneous frequency estimation using robust spectrogram with varying window length,” *AEU International Journal of Electronic Communications*, Vol. 54, No.4, pp. 193-202.
- [23] I. Djurović and LJ. Stanković, “Robust Wigner distribution with application to the instantaneous frequency estimation,” *IEEE Trans. Sig. Proc.*, Vol. 49, No.12, Dec. 2001, pp. 2985-2993.
- [24] S. Barbarossa and V. Petrone, “Analysis of polynomial-phase signals by the integrated generalized ambiguity function,” *IEEE Trans. Sig. Proc.*, Vol. 45, No. 2, Feb. 1997, pp. 316-327.
- [25] P. O’Shea, “A fast algorithm for estimating the parameters of a quadratic FM signal,” *IEEE Trans. Sig. Proc.*, Vol. 52, No. 2, Feb. 2004, pp. 385-393.
- [26] I. Djurović and LJ. Stanković, “Realization of the robust filters in the frequency domain,” *IEEE Sig. Proc. Lett.*, Vol. 9, No. 10, Oct. 2002, pp. 333-335.
- [27] X. Guo, H.-B. Sun, S.-L. Wang and G.-S. Liu, “Comments on “Discrete chirp-Fourier trans-

- form and its application to chirp rate estimation", *IEEE Trans. Sig. Proc.*, Vol. 50, No.12, Dec. 2002, p. 3115.
- [28] X.-G. Xia, "Response to "Comments on 'Discrete chirp-Fourier transform and its application to chirp rate estimation'", *IEEE Trans. Sig. Proc.*, Vol. 50, No.12, Dec. 2002, p. 3116.
- [29] D. L. Donoho and P. J. Huber, "The notion of breakdown point," *E.L. Lehmann Festschrift*, Bickel, P.J., K. Doksum and J.L. Hodges, Jr. (eds.), Wadsworth Press.
- [30] S. Peleg and B. Friedlander, "The discrete polynomial-phase transform," *IEEE Trans. Sig. Proc.*, Vol. 43, No.8, Aug. 1995, pp. 1901-1914.
- [31] S. Peleg and B. Porat, "Linear FM parameter estimation from discrete time observations," *IEEE Trans. Aerosp. Electron. Syst.*, Vol. 27, No.4, July 1991, pp. 607-616.
- [32] S. Peleg and B. Porat, "The Cramer-Rao lower bound for signals with constant amplitude and polynomial phase", *IEEE Trans. Sig. Proc.*, Vol. 39, No.3, Mar. 1991, pp. 749-752.
- [33] G. R. Arce, "A general weighted median filter structure admitting negative weights," *IEEE Trans. Sig. Proc.*, Vol. 46, No. 12, Dec. 1998, pp. 3195-3205.
- [34] H. Krim and I. C. Schick, "Minimax description length for signal denoising and optimized representation," *IEEE Trans. Inf. Th.*, Vol. 45, No. 2, pp. 898-908, Apr. 1999.
- [35] C. L. Nikias and M. Shao, *Signal processing with alpha stable distributions and applications*, Wiley 1995, New York.
- [36] X. Wang and H. V. Poor, "Robust multiuser detection in non-Gaussian channels," *IEEE Trans. Sig. Proc.*, Vol. 47, No.2, Feb. 1999, pp. 289-305.
- [37] A. Taguchi: "Adaptive a-trimmed mean filter with excellent-detail preserving," in *Proc. of ICASSP 1994*, Vol. 5, pp. 61-64, 1994.
- [38] I. Djurović, V. V. Lukin: "Filtering of frequency modulated signals in impulse noise environments based on robust DFT forms," in *Proc. of SMMSP 2004*, 2004, Vienna, Austria, pp.95-100.